

Theoretical and experimental study on intramolecular charge-transfer in symmetric bi-1,3,4-oxadiazole derivatives



Haitao Wang^{a,b}, Huimin Liu^a, Fu-Quan Bai^b, Songnan Qu^c, Xiaoshi Jia^a, Xia Ran^a, Fangyi Chen^a, Binglian Bai^d, Chengxiao Zhao^a, Zibai Liu^a, Hong-Xing Zhang^{b,*}, Min Li^{a,*}

^a Key Laboratory of Automobile Materials (MOE) & College of Materials Science and Engineering, Jilin University, Changchun 130012, China

^b Key Laboratory of Theoretical and Computational Chemistry, Institute of Theoretical Chemistry, Jilin University, Changchun 130023, China

^c Key Laboratory of Excited State Processes, Changchun Institute of Optics, Fine Mechanics and Physics, Chinese Academy of Sciences, Changchun 130033, China

^d College of Physics, Jilin University, Changchun 130012, China

ARTICLE INFO

Article history:

Received 18 April 2015

Received in revised form 24 June 2015

Accepted 13 July 2015

Available online 22 July 2015

Keywords:

Intramolecular charge transfer

Fluorescence

1,3,4-oxadiazole

Electronic structure

CAM-B3LYP

ABSTRACT

The photophysical properties of 2,2'-bis-(4-alkoxyphenyl)-bi-1,3,4-oxadiazole (BOXD-*n*), have been studied by a combination of spectroscopic techniques and theoretical calculations. Interestingly, strong fluorescence red-shift in polar solvents was observed in this highly symmetric molecule, which indicates an efficient charge transfer (CT) occurred in the excited state. The change of molecular dipole moment between the ground state and CT excited state was calculated to be 9.9 D. Theoretical calculations at Density Functional Theory level revealed that the first singlet excited state of BOXD-*n* shows both π - π^* and CT characters. Clear evidence for charge transfer from alkoxy benzene to the central bi-1,3,4-oxadiazole group can be observed by analysing the atomic charge and electron density change, though it is not significant. Since BOXD-1 retained a planar conformation and became more quinoid-like in the excited state, a planar intramolecular charge transfer is assigned for it. By further comparing these results with the half molecule terminated by $-\text{CH}_3$ group (2-tetradecyloxyphenyl, 5-methyl-1,3,4-oxadiazole), it could be concluded that intramolecular charge transfer property was enhanced in this DAAD arrangement of BOXD-*n*.

© 2015 Elsevier B.V. All rights reserved.

1. Introduction

Intramolecular charge transfer (ICT) is one of the most widely studied phenomena in the photophysics of donor (D)-acceptor (A) π -conjugated systems [1,2]. Since the first observation of ICT phenomenon in 4-*N,N'*-dimethylaminobenzonitrile (DMABN) by Lippert et al. [3], many ICT-based aryl amines have been designed and synthesized for potential applications in chemical sensors, fluorescence probe, and the mimicry of photosynthesis in plants [1,4–9].

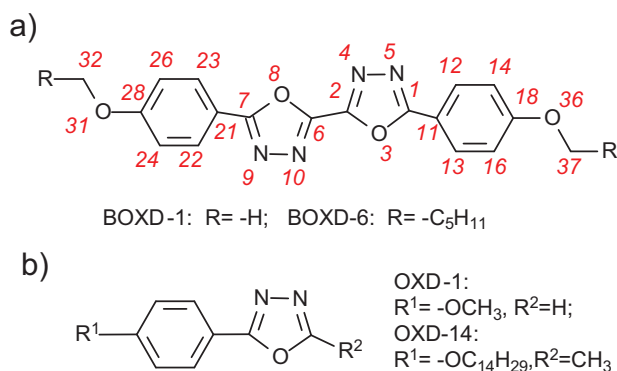
However, the mechanism for the ICT is very versatile, even controversial in some systems [1]. There is a heated debate over molecular conformation change in the ICT process, the two dominant models being the twisted intramolecular charge transfer (TICT) and planar intramolecular charge transfer (PICT) [1,10].

According to the TICT model, electron transfer from the donor to the acceptor moiety occurs in the completely twisted molecular structure, the donor group is perpendicular to the rest of the molecule. In this configuration, complete decoupling of the groups leads to full charge transfer and a large dipole moment. Thus, greater stabilization is achieved in solvents of higher polarity [1]. The PICT hypothesis is based on the equilibrium dynamics between the local excited state (LE) and ICT state, which takes place on a picosecond timescale [1,10]. The PICT model postulates an ICT structure with an increased double bond character between donor and acceptor moieties, resulting in a quinoidal resonance structure [10]. In addition to TICT and PICT hypothesis, rehybridised intramolecular charge transfer (RICT) and wagging intramolecular charge transfer (WICT) models have also been proposed for some special systems [1].

The extensively investigated ICT systems are those molecules having a D- π -A structure, which all possess a large molecular dipole. Other systems, especially molecules with a symmetric structure, have not yet been studied in detail. Interestingly, we have observed emission spectra from a CT state in a series of

* Corresponding authors. Tel.: +86 43185168254.

E-mail addresses: zhanghx@mail.jlu.edu.cn (H.-X. Zhang), minli@mail.jlu.edu.cn (M. Li).



Scheme 1. The molecular structure of BOXD-*n* and OXD-*n*. The atomic number used in calculations and the text below is shown in BOXD-1.

highly symmetric molecules, 2,2'-bis-(4-alkoxyphenyl)-bi-1,3,4-oxadiazole (denoted as BOXD-*n*, *n* indicates the number of carbon atoms in the alkoxy chains, see Scheme 1a). A similar phenomenon was also observed in other 1,3,4-oxadiazole derivatives, but the mechanism for it has not been illustrated [11,12]. The synthesis of BOXD-*n* has been reported previously [13]; in our present work, we focus on the photophysical properties, especially the ICT mechanism for BOXD-*n*. A combination of spectroscopic studies and theoretical calculations were carried out to provide insight into the nature of ICT in these systems.

2. Materials and methods

2.1. Experimental details

The synthesis of BOXD-6 was reported previously. The purity of material (BOXD-6) was verified by FT-IR, ¹H NMR and Elemental analysis [13]. All the solvents for spectral measurements were of spectroscopic grade and used as received. The following abbreviations are used throughout the text: cyclohexane, CHEX; chloroform, CHL; tetrahydrofuran, THF; acetonitrile, ACN; ethanol, ETO; methanol, MTO. UV-vis absorption spectra were obtained using a Shimadzu UV-2550 spectrometer. Photoluminescence spectra were collected by a Perkin-Elmer LS55 spectrophotometer. The room-temperature luminescence quantum yields in solutions were determined relative to quinine sulfate in sulfuric acid aqueous solution (0.546), and calculated according to the following equation: $\Phi_{\text{unk}} = \Phi_{\text{std}}(\text{Grad}_{\text{unk}}/\text{Grad}_{\text{std}})(n_{\text{unk}}/n_{\text{std}})^2$, where Φ is the quantum yield; Grad is the slope of the straight line by fitting the plot of integrated fluorescence intensity vs absorbance; and *n* is the indexes of refraction of the solutions (pure solvents were assumed); and the subscript unk and std indicate the sample and the standard, respectively [14]. In order to minimize re-absorption effects, absorbance in the 10 mm fluorescence cuvette were controlled under 0.1 at and above the excitation wavelength. Fluorescence lifetimes were measured using FL920 time-correlated single photon counting (TCSPC) system.

2.2. Computational details

In calculation, the hexyloxy group (-OC₆H₁₃) of BOXD-6 was replaced by a methoxy group (BOXD-1, Scheme 1a) to save the computational time. In order to test the reliability of this replacement, we have calculated the excitation energy of BOXD-6 and BOXD-1 with TD-CAM-B3LYP method (CAM-B3LYP/6-311+G**). The excitation energy of BOXD-6 is 4.18 eV in the gas phase and 4.08 eV in CHEX solution, which shows the difference of only 0.02 eV to BOXD-1 (4.20 and 4.10 for BOXD-1 in gas and CHEX phase, respectively), confirming the replacement is safe. The molecular geometries of

BOXD-1 in the ground and excited state were optimized at DFT and TD-DFT level, respectively; then the vertical excitation and emission energies were computed by TD-DFT approach. The bulk solvent effect was considered in each step by using a well-known Polarizable Continuum Model (PCM) [15]. All geometry optimization calculations were performed with equilibrium linear-response PCM (LR-PCM) approach [15], while the TD-DFT energy calculations were performed with non-equilibrium LR-PCM or state-specific PCM (SS-PCM) approaches [16]. SS-PCM was expected to have a better description of solvent effect on this charge-transfer system. The calculated vertical transitional energies were compared with absorption or emission maxima to check the reliability of these method. Although this comparison is non-physical scheme consisting, it has a practical advantage: such calculations are much faster and are used in the large majority of TD-DFT works [17–19].

In order to select a proper method for this system, two different groups of hybrid functionals, namely global hybrid (GH) and range-separated hybrid (RSH) functionals have been tried. For the GH functionals, the percentage of Hartree-Fock exchange (HFE) is constant at each point in space. In the present work, several GHs have been selected: B3LYP (20% of HFE) [20], B3P86 (20% of HFE) [20,21], PBE0 (25% of HFE) [22], BMK (42% of HFE) [23], BH&HLYP (50% of HFE) [24]. For RSH functionals, the fraction of HFE increases as the inter-electronic distance increases, giving the so called long range correction scheme (LC). This group includes CAM-B3LYP approach, where the HFE percentage smoothly increases from 19 to 65% [25], and the LC- ω PBE in which the percentage of HFE ranges between 0 and 100% [26]. In all calculations, standard 6-311+G** basis sets was applied. All these calculations were carried out with Gaussian 09 software package (version D.01) [27].

3. Results and discussion

3.1. Spectroscopic study

Although the UV-vis absorption and fluorescence spectra of BOXD-6 in non-polar cyclohexane (CHEX) has been reported in our previous work [13]; here for the sake of comparison, they are also included.

3.1.1. Absorption spectra

BOXD-6 shows good solubility in various organic solvents of different polarity, which facilitates the experimental study of solvatochromism. As shown in Fig. 1 and Table 1, in dilute solutions ($\sim 10^{-5}$ M), BOXD-6 shows an intense absorption at around 320 nm, as well as a weak band at 250 nm. The high absorption intensity

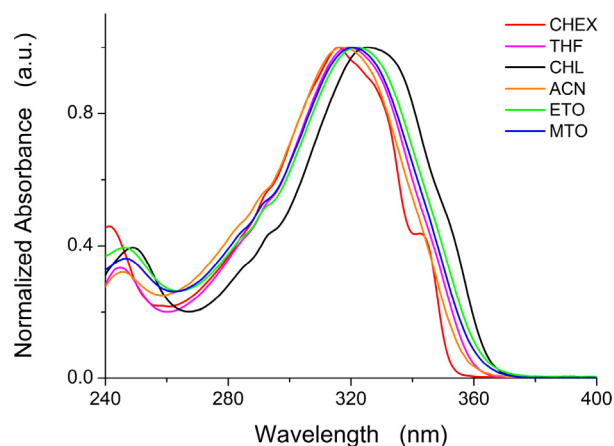


Fig. 1. UV-vis absorption spectra of BOXD-6 (normalized) in different solvents ($\sim 10^{-5}$ M).

Table 1
Photophysical characteristics of BOXD-6 in different solvents ($\sim 10^{-5}$ M) at room temperature.^a

Solvent	ϵ	λ_{abs} (nm)	λ_{em} (nm)	$\Delta\nu_{\text{st}}$ (cm^{-1})	Φ	τ (ns)/ χ^2	k_r ($\times 10^8 \text{ s}^{-1}$)	k_{nr} ($\times 10^8 \text{ s}^{-1}$)
CHEX	2.02	316	370	4619	0.82	0.94/1.04	8.7	1.9
CHL	4.89	325	390	5128	0.49	1.13/0.94	4.3	4.5
THF	7.58	319	386	5441	0.57	1.1/0.89	5.2	3.9
ACN	35.94	320	400	6250	0.75	1.46/1.02	5.1	1.7
ETO	24.55	322	411	6725	0.80	1.75/0.88	4.5	1.1
MTO	32.66	320	419	7384	0.65	2.14/0.82	3.0	1.6

^a ϵ is the dielectric constant; λ_{abs} and λ_{em} indicate the wavelength of maximum absorption and emission, respectively; $\Delta\nu_{\text{st}}$: Stokes shift; Φ : quantum yield; τ : lifetime; k_r : radiative constant; k_{nr} : non-radiative constant.

of the longer-wavelength band indicates that it is a π - π^* type of transition, which is consistent with the result obtained in computational study (see below). The position of the absorbance maximum is slightly dependent on the polarity of the solvents; from CHEX to acetonitrile (ACN) and methanol (MTO), it red-shifts only about 10 nm in wavelength (Fig. 1 and Table 1). This indicates that the electronic and structural nature of the ground and Franck–Condon (FC) excited states, which are responsible for absorption, do not vary much during excitation.

3.1.2. Fluorescence spectra

Fluorescence spectra of BOXD-6 in various solvents are shown in Table 1 and Fig. 2. In non-polar CHEX, BOXD-6 showed an intense emission at around 370 nm with vibrational fine structure (351, 370, and 386 nm, Fig. 2). The fine structures are somewhat retained in solvents with moderate polarity (chloroform (CHL) and tetrahydrofuran (THF)), and are totally lost in the highly polar solvents (ACN, ethanol (ETO) and MTO). These observations indicated the existence of strong solute–solvent interactions in the polar solvents, which broaden the vibronic transitions, thus make the fine structure lost. Moreover, the emission spectra exhibit a large red-shift in their maxima with increasing solvent polarity (Table 1 and Fig. 2). This indicates that due to a charge transfer process, the molecular dipole moment (in this case, the local dipole moment of BOXD-6, as will be discussed below) in the excited state is larger than the ground state.

In order to reveal the polarity effect on the molecular excited state relaxation and the fluorescence spectra in detail, the PL spectra of BOXD-6 were measured in mixed solvents. As shown in Fig. 3A, by titrating CHL into dilute CHEX solution of BOXD-6 ($\sim 10^{-5}$ M), the band shifted to longer wavelength. Although vibrational fine structures were significantly lost, they could still be identified. These observations suggest that although the fluorescence spectra red-shifted with increasing solvent polarity; the

photo-luminescence process in CHEX and CHL are largely the same. The situation for mixing CHEX solution with ETO is different. The former two peaks (351, 370 nm) decreased with a little amount of ETO, while the peak at 386 nm increased in relative intensity, and became dominant as the ratio of ETO to CHEX reached about 5% (see Fig. 3B). This fact that the emission band position is so sensitive to the solvent polarity (with a little amount of polar solvent) indicated strong charge transfer character of the excited state for BOXD-6. The change of peak shape in the case with CHEX/ETO mixed solvent might be due to not only the charge transfer, but also specific intermolecular interactions, for example hydrogen bonding, as usually observed in the CT systems [6].

3.1.3. Solvatochromic measurements and dipole moments

The Stokes shifts ($\Delta\nu_{\text{st}}$) of BOXD-6, calculated from the maxima of the absorption and fluorescence spectra, are shown in Table 1. The Stokes shifts provide a measure of energy difference between the Franck–Condon (FC) and CT excited states. From CHEX to MTO, the values of Stokes shift are in a range of 4600–7000 cm^{-1} (Table 1), and increase along with increasing solvent polarity, indicating that the CT state can be stabilized with polar solvents.

The change in the dipole moment ($\Delta\mu_{\text{ge}}$) between the CT excited state (μ_{CT}) and the ground state (μ_{g}) can be calculated from Lippert–Mataga equation (Eq. (1)), i.e., from linear variation of Stokes shift ($\Delta\nu_{\text{st}}$) against the solvent parameters, $\Delta f(\epsilon, n)$ (Eq. (2)) [28,29].

$$\Delta\nu_{\text{st}} = \frac{2}{(4\pi\epsilon_0)(hca^3)} \times (\mu_{\text{CT}} - \mu_{\text{g}})^2 \times \Delta f(\epsilon, n) + \text{Const.} \quad (1)$$

$$\Delta f(\epsilon, n) = \frac{\epsilon - 1}{2\epsilon - 1} - \frac{n^2 - 1}{2n^2 + 1} \quad (2)$$

where $\Delta\nu_{\text{st}}$ is the Stokes shift; h is the Planck's constant; c is the velocity of light, μ_{CT} is the dipole moment of the CT excited state; μ_{g} is the dipole moment of the ground state; a , the solvent cavity (Onsager) radius was obtained by optimizing the molecular geometry of BOXD-6 at the CAM-B3LYP/6-311+G** level of theory; ϵ and n are the dielectric constant and refractive index of the solvent, respectively. We obtained $\Delta\mu_{\text{ge}} = 9.9$ D for BOXD-6 from the relationship between the Stokes shifts values and the solvation parameters (Fig. 4). The relatively larger change in the dipole moment is a direct evidence for the CT character of the excited state.

3.1.4. Quantum yields and fluorescence decay

The fluorescence quantum yields (Φ) and lifetimes (τ) for BOXD-6 in different solvents have been measured and the data are also collected in Table 1. BOXD-6 shows very high quantum yield in most solvents (>50%). The value of Φ decreases with the increasing polarity, suggesting that the elongation of molecular relaxation process (or time) in the polar solvent, as has been confirmed by relatively larger Stokes shifts and longer life time below, may promote the probability of non-emissive de-active process.

In order to get more information about the excited state decay, we have measured time-resolved photoluminescence decay dynamics of BOXD-6 in different solutions using the time correlated

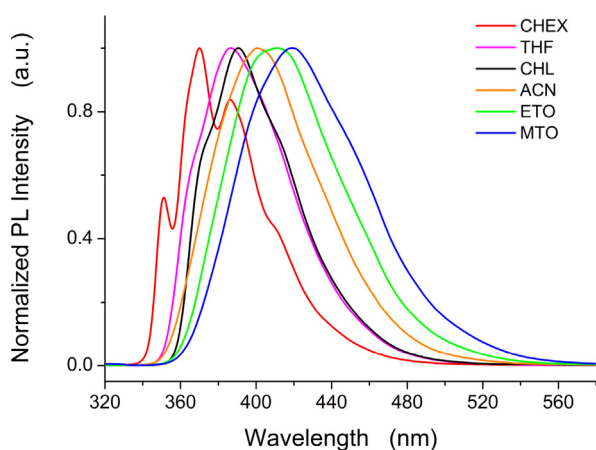


Fig. 2. Fluorescence spectra of BOXD-6 (normalized) in different solvents ($\sim 10^{-5}$ M).

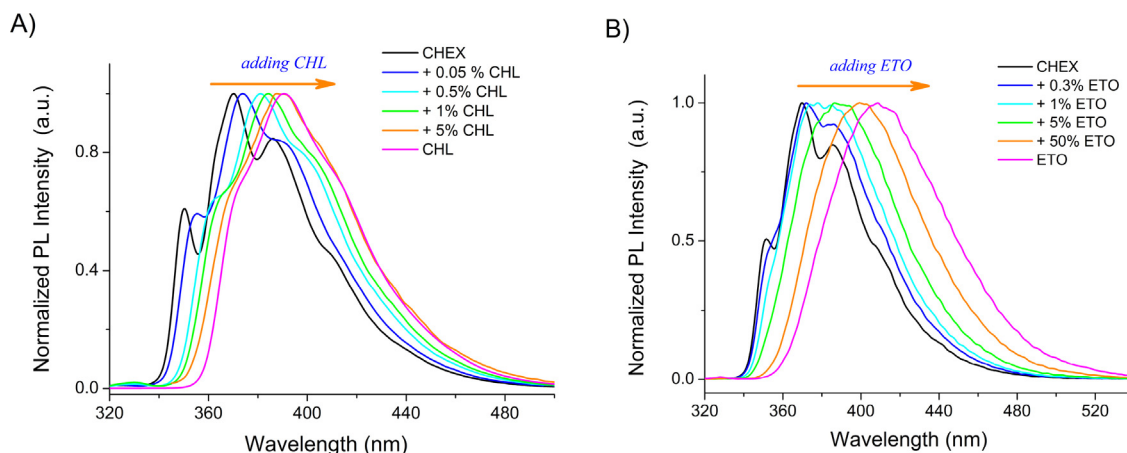


Fig. 3. Fluorescence spectra of BOXD-6 in mixed solvents, (A) mixing CHEX with CHL and (B) mixing CHEX with ETO.

single photon counting (TCSPC) method. All these fluorescence decays could be well fitted by a single-exponential function and lifetimes in the range of 0.94–1.46 ns in aprotic solvent, 1.75 ns in ETO and 2.14 ns in MTO were observed (Table 1). The increase of the fluorescence decay time with increasing solvent polarity indicates that the excited state could be stabilized in polar solvents, thus the processes for rearrangement of electronic excited states and the solvent molecules can take place. The extremely long decay time in ETO and MTO might indicate that specific solute-solvent interaction was involved in the excited state [6], as has been revealed in the static fluorescence spectroscopic studies. The calculated radiative constants (k_r) and non-radiative constants (k_{nr}) indicated that in polar protic solvents a decrease of k_r is the main effect, whereas the change in k_{nr} is minor (Table 1). This can also confirm the specific solute-solvent interaction.

3.2. Theoretical study

3.2.1. Electronic state transitions

Theoretical calculations at DFT level were carried out to reveal the physical picture of the electronic excitation, excited state molecular geometry and the light emission processes. To save the computational time, the hexyloxy group ($-\text{OC}_6\text{H}_{13}$) of BOXD-6 was replaced by a methoxy group ($-\text{OCH}_3$, BOXD-1, Scheme 1a and Fig. S1). It should be noted that one excited state may consist of different orbital transitions base on different functionals (Table S1).

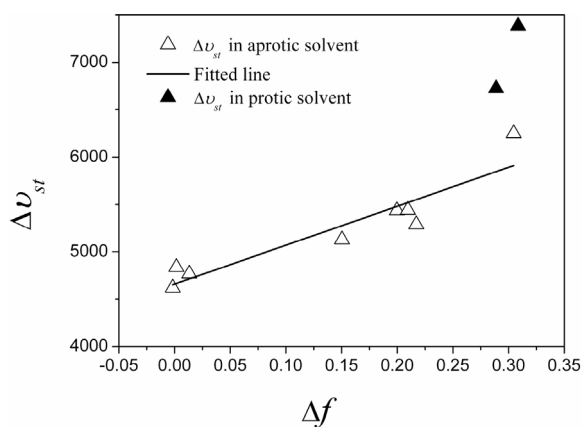


Fig. 4. Plot of Stokes shift ($\Delta\nu_{st}$, cm^{-1}) against the solvent polarity parameters for BOXD-6. The Stokes shift ($\Delta\nu_{st}$) can be fitted with a linear line ($R^2=0.85$).

Table 2 lists the excitation energy and oscillator strengths of the five lowest electronic transitions of BOXD-1 calculated with different functionals. All these methods reveal that S_0 to S_1 transition is highly allowed. Other allowed transitions (non-zero oscillator strengths) were the S_0 – S_4 transition by using global hybrid (GH) functionals, with a percentage of HFE below 50%; or the S_0 – S_3 transition by functionals with HFE above 50%. Transitions calculated using range-separated hybrid (RSH) functionals predicted that the S_0 – S_3 and S_0 – S_5 transitions had non-zero oscillator strength. All these results indicated that the two main peaks observed in the UV–vis absorption spectra can be attributed to the transitions from ground state to S_1 and higher excited states, respectively.

It is interesting to find that, as expected, increasing the HFE ratio in the GHs functionals yields larger excitation energies and oscillator strength (Table 2), which ranges from 3.54 eV (B3LYP, $f=1.182$) to 4.30 eV (BH&HLYP, $f=1.520$). Even higher energy was found with LC- ω PBE (4.63 eV, $f=1.619$), while the CAM-B3LYP and M062x approaches show an intermediate behavior between BMK and BH&HLYP. The inclusion of solvent effects (CHEX) by a LR-PCM approach gave a red-shift of these excitation energies. As compared with the experimental result, the best agreement is found with BMK, CAM-B3LYP and M062x approaches (within 0.25 eV); the excitation energy delivered by B3LYP is extremely lower than experimental data (over 0.5 eV). Considering the excellent performance of CAM-B3LYP approach in current study and other charge transfer systems, it was applied to explore the mechanism of charge transfer in BOXD- n .

Fig. 5 presents the electronic density of frontier molecular orbitals of BOXD-1 involved in the five lowest transitions. As can be seen, all the occupied orbitals consist mainly of π -bonding orbitals within each aromatic ring (benzyl and 1,3,4-oxadiazole rings), except for orbital H-6 and H-5, which are contributed by the n orbital of N atoms. On the contrary, the unoccupied orbitals are mainly composed of the π -antibonding orbitals, or π -bonding between aromatic rings. In addition, the wave functions are perfectly delocalized over the whole π -system for orbital H-4, HOMO and L+2, while other orbitals are somewhat showing localized properties. Orbital H-6, H-5 and LUMO have the electron density localized on the bi-1,3,4-oxadiazole unit (acceptor), while others localized on the methoxy phenyl rings (donor).

As mentioned above, according to the TD-CAM-B3LYP calculations, the three lowest allowed transitions are $S_1 \leftarrow S_0$ (4.2 eV, $f=1.520$), $S_3 \leftarrow S_0$ (4.97 eV, $f=0.020$) and $S_5 \leftarrow S_0$ (5.46 eV, $f=0.001$). An inspection of the component orbital transitions make it clearer that the former two absorptions should be assigned as a π – π^* type, where the first one is highly allowed and mainly consist of $H \rightarrow L$,

Table 2
Computed excitation energy (in eV) and oscillator strengths (in parenthesis) for the five lowest excited states of BOXD-1.

Model	S_1		S_2	S_3	S_4	S_5
	GAS	CHEX				
B3LYP	3.54 (1.182)	3.41 (1.258)	4.03 (0)	4.45 (0)	4.55 (0.038)	4.60 (0)
B3P86	3.56 (1.211)	3.44(1.290)	4.07 (0)	4.50 (0)	4.60 (0.035)	4.65 (0)
PBE0	3.70 (1.296)	3.58(1.329)	4.29 (0)	4.62 (0)	4.72 (0.039)	4.77 (0)
BMK	4.16 (1.456)	4.04 (1.553)	4.82 (0)	4.97 (0)	4.98 (0.033)	5.21 (0)
BH&HLYP	4.30 (1.520)	4.19(1.621)	4.98 (0)	5.15 (0.020)	5.16 (0)	5.57 (0)
CAM-B3LYP	4.20 (1.520)	4.10 (1.625)	4.87 (0)	4.97 (0.020)	4.98 (0)	5.46 (0.001)
LC- ω PBE	4.63 (1.619)	4.54(1.750)	5.16 (0)	5.17 (0.016)	5.20 (0)	5.83 (0.002)
M062x	4.28 (1.525)	4.17 (1.633)	4.94 (0)	5.02 (0.026)	5.03 (0)	5.53 (0)
Expt.		3.93				

H-1 \rightarrow L+1 and H-4 \rightarrow L transitions, the second one is a combination of several transitions, mainly including H-3 \rightarrow L+1, H-2 \rightarrow L, H-1 \rightarrow L+3, H \rightarrow L+2, and H \rightarrow L+5. Whereas the third absorption is an $n-\pi^*$ type, containing H-6 \rightarrow L, H-6 \rightarrow L+2, H-6 \rightarrow L+4, and H-5 \rightarrow L+1 transitions. So, the lower-energy absorption band should show only $\pi-\pi^*$ character, while the higher energy band may consist both $n-\pi^*$ and $\pi-\pi^*$ type of transitions. Inclusion of the CHEX solvent by PCM model shows little influence on the lowest absorptions but has changed the order of the higher level excited states, for it increases the excitation energy for the $n-\pi^*$ transitions, while decreases the $\pi-\pi^*$ transition energy (Table S2). Further increasing the solvent polarity shows little influence on these absorption transitions, neither the excitation energy nor the component orbital transitions for each excited state changed, even with the molecular

geometries optimized with the solvents (Table S2), implying that the electronic and structural nature of BOXD-1 is not sensitive to the solvent polarity in the ground and FC excited states. The lack of structural and electronic sensitivity towards solvents is consistent with the low correlation between absorbance behavior and solvent observed experimentally.

In order to get a direct view on the extent of the charge transfer for each excited state, maps of the electron density variation from S_0 to S_1 , S_3 , and S_5 are presented in Fig. 6. From S_0 to S_1 , the variation of the electron density is spread over the whole molecule, including both $\pi-\pi^*$ and CT characters (Fig. 6a). The electron density change over methoxy group is mainly negative; for phenyl group, the negative domain is slightly larger than positive domain; on the contrary, for bi-oxadiazole group, the area of positive domain is obviously

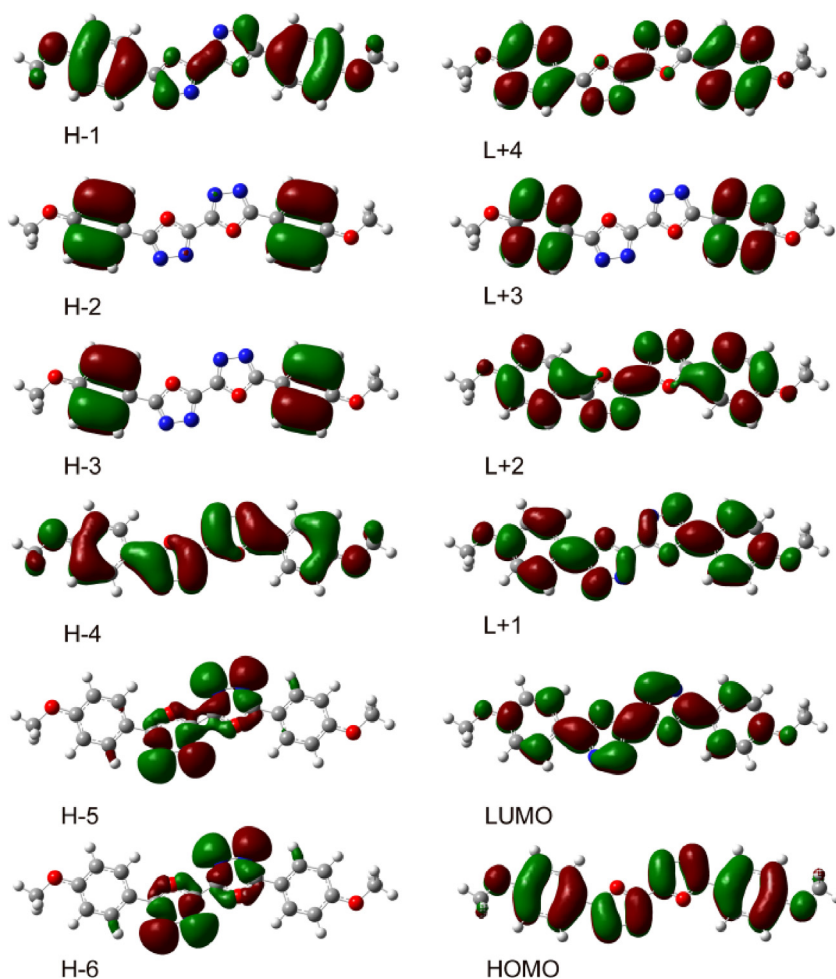


Fig. 5. Electron density diagrams of molecular orbitals of BOXD-1 computed with CAM-B3LYP/6-311+G** method.

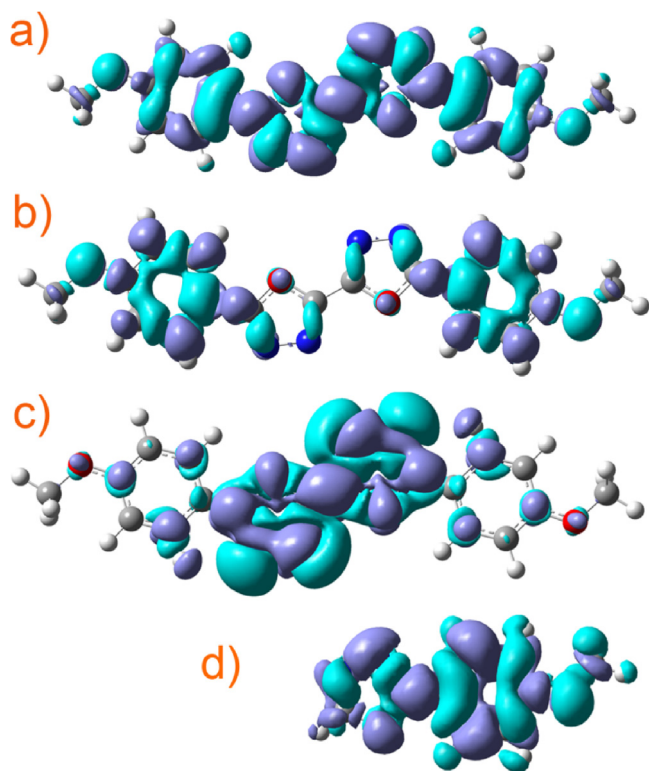


Fig. 6. Electron density difference between the ground and excited states: (a–c) for BOXD-1, S_0 – S_1 , S_0 – S_3 , and S_0 – S_5 , respectively; (d) for OXD-1, S_0 – S_1 (at ground state geometries, purple positive, cyan negative).

larger than that of negative domains, indicating clearly that electron has been transferred from side methoxy and phenyl group to central bi-oxadiazole group. By further calculating the surface area of each group in positive or negative only plot of the electron density difference (Fig. S2), it revealed that the surface area of OXD group showed a net increase of about 6% of total surface area, while BEN and MET group showed a net decrease of 4% and 2%, respectively. The variation in S_0 – S_3 and S_0 – S_5 transitions are mainly localized, with only a little charge transfer character (Fig. 6b and c). For S_0 to S_3 , the variation is localized on side methoxy benzene, while in the case of S_0 to S_5 , it is localized on central bi-1,3,4-oxadiazole group. Considering the calculation method, the electron density we have calculated is for the Frank–Condon excited states, so it could be concluded that only a small amount of electron was transferred during the photo-excited process. This may be the reason for the little red-shift was observed in the UV–vis absorption spectra.

3.2.2. Excited state geometry and ChelpG charges

Additional information on the nature of excited state can be obtained by analysing the molecular geometry, charge distribution, and dipole moment of these excited states. The molecular geometry for BOXD-1 in its five lowest singlet excited states (according to excitation energy) was optimized with TD-CAM-B3LYP approach, which yield planar structure for each state (Fig. S1) of similar energies (Table 3, in the order of increasing excitation energy). Even when the molecular geometry was optimized initially with a twisted molecular structure (with both dihedral angles $N9$ – $C7$ – $C21$ – $C22$ and $N5$ – $C1$ – $C11$ – $C12$ equalling 30°) or without any symmetry constraint, a planar structure was obtained.

The atomic charges for the ground state and the first excited state of BOXD-1 were calculated with an electrostatic potential model (ChelpG) at CAM-B3LYP/6–311+G** level (Table S3), which was demonstrated to have better performance [30]. On the ground

Table 3

TD-CAM-B3LYP/6–311+G** adiabatic energies (ΔE), vertical emission energies (E_{em}) and oscillator strengths (f) for the five lowest singlet excited states of BOXD-1 in the gas phase.

Excited State	ΔE^a (kcal/mol)	E_{em} (eV)	Oscillator strength
S_1	0	3.43	1.57
S_2	3.56	3.83	1.59
S_3	7.24	4.06	1.54
S_4	6.96	4.05	1.53
S_5	4.48	3.51	1.57

^a Adiabatic minimum energy relative to the S_1 state (–1213.9115345 au).

state, the 1,3,4-oxadiazole ring (OXD) and benzyl ring (BEN) possess a positive charge of 0.079, and 0.108 |e|, respectively, while the methoxy group (MET) possesses a negative charge of –0.187 |e|. When going to the S_1 state, the charge value of the OXD moiety decreased, while that of the BEN and MET group increased (Fig. 7), indicating that electron (about 0.02 |e|) was transferred from the side methoxy benzene (donor) to the central bi-1,3,4-oxadiazole ring (acceptor) under electronic excitation. So, the charge transfer parameter, which is defined as $f_{CT} = \Delta q_D - \Delta q_A$, where Δq_i is the charge difference in the donor or acceptor unit between ground and excited state, is calculated as 0.04 |e| [10]. The net amount of charge transferring to OXD group is slightly affected by involving the solvent or increasing the polarity of the solvent, whereas much more obvious influence of solvent on the BEN and MET group could be observed (Fig. 7). The net amount of charge transferring from BEN group decreases, while that from the MET group increases with the increasing polarity of the solvent. It means that although the net amount of transferred charge does not vary a lot by the solvent, the charge transfer length increases by involving the solvent or increasing the polarity. It should be noted that the calculated atomic charges are only approximate, so we could not get the exact net amount of charge transferred; however, our present work has shown a correct trend. Small net charge was also reported for the charge transfer state of PICT nature [10]. Although the charge transfer revealed by these theoretical calculations can indeed strengthen the local dipoles in BOXD-1 (for half molecule), these local dipoles cancelled out each other due to a symmetric arrangement of them. So the calculated dipole moment of the whole BOXD-1 molecule did not show any change. The enhanced dipole moment observed in the experimental study should be attributed to the local dipole.

To get direct information on the intramolecular charge transfer mechanism, a TD-CAM-B3LYP rigid scan of the twisting angle between donor and acceptor moieties (dihedral angle) has been carried out. As shown in Fig. 8, the energy goes up when the twisting angle increases from 0 to 90° . The activation barrier is about 7.5 kcal/mol. This behaviour is different from the model TICT compound (DMABN), which can yield a second energy minimum state

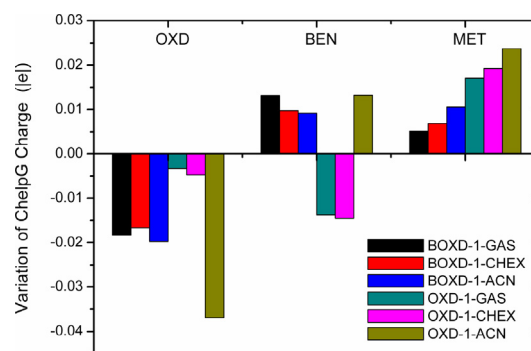


Fig. 7. Variation of sum of ChelpG charge for OXD, BEN and MET moieties of BOXD-1 and OXD-1 in the excited states compared to the ground state, computed with CAM-B3LYP/6–311+G** method.

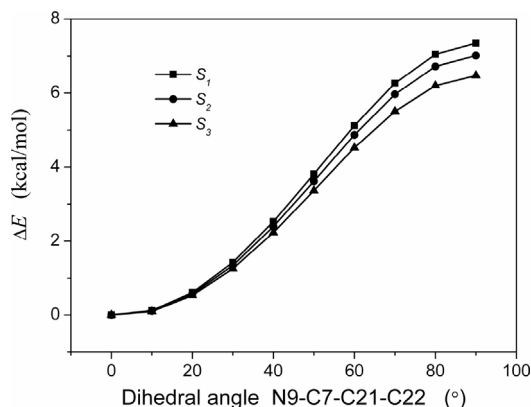


Fig. 8. Relative energy profiles of excited state of BOXD-1 with respect to the planar structure obtained in a rigid scan of the dihedral angle N9–C7–C21–C22, computed with CAM-B3LYP/6–311+G** method.

along the twisting coordinates, so a PICT mechanism should be assigned for BOXD-*n*. Moreover, The bond length of C1–C11 and C2–C6 which connect the aromatic rings, and C12–C14, C13–C16, C18–O36 bonds which are conjugated with C1–C11 and C2–C6 decreases during the electronic excitation, while other bonds are on the contrary, lengthening during this process (Fig. 9), indicating that BOXD-1 becomes more quinoid-like in the excited state.

3.2.3. Computed emission energy

Based on these optimized excited state molecular geometries, the emission energy of BOXD-1 were also calculated with TD-CAM-B3LYP/6–311+G** method. As shown in Table 3 and Table S3, the calculated vertical emission energy of the S_1 state is 3.43 eV in gas phase. Inclusion of CHEX as the solvent by a non-equilibrium LR-PCM approach (with the geometry obtained in gas phase) can make the emission energy red-shift about 0.13 eV, which is in excellent agreement with the emission maximum of the fluorescence in CHEX (3.35 eV). However, further increase the solvent polarity showed very slight influence on the emission spectra (red-shift 0.01 eV, Table S3). As shown in Fig. 10, when the emission energies were plotted against the solvent parameters, $\Delta f(\epsilon, n)$, the slope for the computed emission energy is very small, which is in contrary to the experimental observations. The vertical emission energy calculated with a non-equilibrium LR-PCM approach base on an equilibrium molecular geometry optimized in solvent fields can give a solvatochromic trends qualitatively consistent with the experimental results. A better description of the solvent effect can be obtained with a non-equilibrium SS-PCM approach, in which, from CHEX to ACN, the emission energy red-shifted by

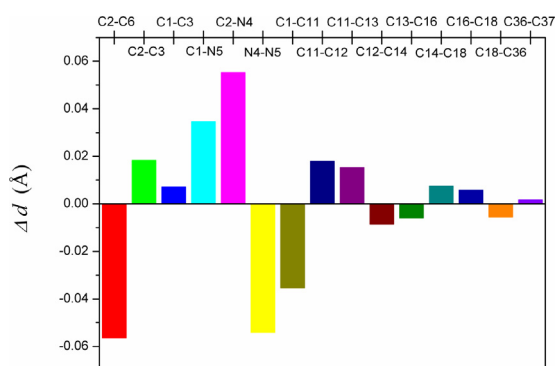


Fig. 9. Variation of bond lengths of BOXD-1 going from S_0 to S_1 state, computed with CAM-B3LYP/6–311+G** method.

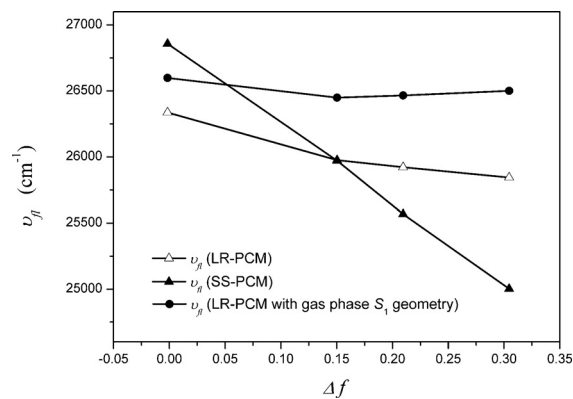


Fig. 10. Plot of computed vertical emission energy (TD-CAM-B3LYP/6–311+G**) vs. solvent parameter Δf for BOXD-1. The S_1 geometry is optimized in the gas phase or corresponding solvent with an equilibrium LR-PCM approach; the emission energy was calculated with a non-equilibrium LR- or SS-PCM approach.

0.23 eV (about 30 nm), in excellent agreement with the experimental observation (Table S3 and Fig. 10).

It is much clearer that the lowest singlet excited state of BOXD-*n* includes both π - π^* and CT characters. The CT character is not very significant, only small amount of electron was transferred during the photo-excitation process. The red-shift of the emission spectra is due to the molecular geometry relaxation in solutions and reorganization of the solvent molecules, as has been confirmed by the fluorescence decay studies.

3.3. The effect of molecular symmetry on ICT properties

It is interesting to found that this highly symmetric molecule with a DAAD arrangement to show ICT property. In order to further discuss the effect of molecular symmetry on ICT property, the half molecule of BOXD-*n* terminated with $-\text{CH}_3$ group (2-tetradecyloxyphenyl, 5-methyl-1,3,4-oxadiazole, denoted as OXD-14, Scheme 1b) was synthesized (the synthesis details can be found in ESI). The absorption and emission spectra of OXD-14 in solvents of varying polarity were measured, and the data was collected in Table S4. OXD-14 showed an intense absorption at around 270 nm, and similarly, the position of this absorbance maximum is slightly dependent on the polarity of the solvents, from CHEX to ACN and MTO, it red-shifts only 4 nm (9 nm for BOXD-6). Under excitation, OXD-14 showed an emission at around 320 nm in CHEX. The emission band red-shifts with the increasing polarity of solvents, however, the extent (about 10 nm) is less than that of BOXD-6 (about 50 nm).

Similar to BOXD-1, further calculations were also carried out on OXD-1 (Scheme 1b) to get insight into the excited state properties. Atomic charge analysis revealed that the amount of transferred charge in OXD-1 during excitation is similar to BOXD-1 in gas phase and CHEX solution (0.02 |e|, Fig. 7); while it was extensively enlarged in ACN (0.04 |e|). However, different from BOXD-1, BEN ring in OXD-1 is behaving as an electron acceptor, rather than an electron donor in gas phase and CHEX; the situation changed in ACN solution, where BEN ring became electron donor as it usually does in BOXD-1, OXD group behaves as the only electron acceptor. This charge transfer could be also confirmed by the electron density change during excitation process (Fig. 6d). In agreement with the experimental observation, the red-shift of the computed vertical emission energy with a SS-PCM approach is about 8 nm on the increasing solvent polarity (Table S4), which is much less than BOXD-1, though relative large amount of transferred charge was observed in OXD-1. These comparisons gave direct evidence that DAAD structure in BOXD-6 enhances the ICT property.

4. Conclusions

The combination of spectroscopic studies and TD-DFT calculations has made the physical picture of the electronic excitation, excited state molecular geometry and light emission process of symmetric bi-1,3,4-oxadiazole derivatives (BOXD-*n*) much clearer. BOXD-6 shows no significant charge transfer character in FC excited state, but shows clear evidence for charge transfer character after excited state geometry relaxation. So the CT excited state shows stronger polarity than the Franck–Condon excited state, which is the reason for the small red-shift in UV–vis absorption spectra, while large red-shift in fluorescence spectra were observed in the polar solvents. Considering the symmetric molecular structure and the charge transfer picture of BOXD-1, the highly polar excited state revealed by the spectroscopic study might be due to the local molecular dipole change (half molecule). TD-DFT calculations based on CAM-B3LYP functionals revealed that S_1 state should be responsible for this light emission, in which the intramolecular charge transfer is observed from the side alkoxy benzene to the central bi-1,3,4-oxadiazole moiety, based on a PICT mechanism. This study provided us an excellent model to consider the effect of molecular symmetry on intramolecular charge transfer; it revealed that the DAAD structure can enhance the ICT property for the first time.

Acknowledgements

Author H.W. would like to thank Dr. Veaceslav Coropceanu, Prof. Jean-Luc Brédas (Georgia Institute of Technology) and Dr. Wenlan Liu (University of Wurzburg) for helpful discussions, Dr. Jian Wang (Jilin University) for providing HPC skills. This work was supported by National Science Foundation of China (51103057, 51073071, 21173096, 21072076, and 21003057), Postdoctoral Science Foundation of China (2012T50294) and Jilin University (200903014).

Appendix A. Supplementary data

Supplementary data associated with this article can be found, in the online version, at <http://dx.doi.org/10.1016/j.jphotochem.2015.07.006>

References

- [1] Z. Grabowski, K. Rotkiewicz, W. Rettig, *Chem. Rev.* 103 (2003) 3899–4031.
- [2] N. Mataga, H. Chosrowjan, S. Taniguchi, *J. Photochem. Photobiol. C: Photochem. Rev.* 6 (2005) 37–79.
- [3] E. Lippert, W. Luder, H. Boos, *Advances in Molecular Spectroscopy*, Pergamon, Oxford, 1962.
- [4] K. Zachariasse, S. Druzhinin, W. Bosch, R. Machinek, *J. Am. Chem. Soc.* 126 (2004) 1705–1715.
- [5] I. Gomez, Y. Mercier, M. Reguero, *J. Phys. Chem. A* 110 (2006) 11455–11461.
- [6] R. Singh, S. Mahanta, S. Kar, N. Guchhait, *Chem. Phys.* 342 (2007) 33–42.
- [7] A. Chakraborty, S. Kar, D. Nath, N. Guchhait, *J. Phys. Chem. A* 110 (2006) 12089–12095.
- [8] B. Kumar Paul, A. Samanta, S. Kar, N. Guchhait, *J. Lumin.* 130 (2010) 1258–1267.
- [9] T. Fujiwara, M.Z. Zgierski, E.C. Lim, *J. Phys. Chem. A* 115 (2011) 586–592.
- [10] C.A. Guido, B. Mennucci, D. Jacquemin, C. Adamo, *Phys. Chem. Chem. Phys.* 12 (2010) 8016.
- [11] S. Varghese, N.S.S. Kumar, A. Krishna, D.S.S. Rao, S.K. Prasad, S. Das, *Adv. Funct. Mater.* 19 (2009) 2064–2073.
- [12] S. Qu, L. Zhao, Z. Yu, Z. Xiu, C. Zhao, P. Zhang, B. Long, M. Li, *Langmuir* 25 (2009) 1713–1717.
- [13] S. Qu, X. Chen, X. Shao, F. Li, H. Zhang, H. Wang, P. Zhang, Z. Yu, K. Wu, Y. Wang, M. Li, *J. Mater. Chem.* 18 (2008) 3954–3964.
- [14] J.R. Lakowicz, *Principles of Fluorescence Spectroscopy*, 3rd ed., Springer, 2006.
- [15] J. Tomasi, B. Mennucci, R. Cammi, *Chem. Rev.* 105 (2005) 2999–3094.
- [16] R. Improta, V. Barone, G. Scalmani, M.J. Frisch, *J. Chem. Phys.* 125 (2006) 054103.
- [17] C. Adamo, D. Jacquemin, *Chem. Soc. Rev.* 42 (2013) 845–856.
- [18] J. Gierschner, J. Cornil, H.J. Egelhaaf, *Adv. Mater.* (2007), 19.173.191.
- [19] D. Jacquemin, V. Wathelet, E.A. Perpète, C. Adamo, *J. Chem. Theory Comput.* 5 (2009) 2420–2435.
- [20] A.D. Becke, *J. Chem. Phys.* 98 (1993) 5648.
- [21] J.P. Perdew, *Phys. Rev. B: Condens. Matter* 33 (1986) 8822.
- [22] C. Adamo, V. Barone, *J. Chem. Phys.* 110 (1999) 6158.
- [23] A.D. Boese, J.M.L. Martin, *J. Chem. Phys.* 121 (2004) 3405.
- [24] A.D. Becke, *J. Chem. Phys.* 98 (1993) 1372.
- [25] T. Yanai, D.P. Tew, N.C. Handy, *Chem. Phys. Lett.* 393 (2004) 51.
- [26] O.A. Vydrov, G.E. Scuseria, *J. Chem. Phys.* 125 (2006) 234109.
- [27] M.J. Frisch, G.W. Trucks, H.B. Schlegel, G.E. Scuseria, M.A. Robb, J.R. Cheeseman, G. Scalmani, V. Barone, B. Mennucci, G.A. Petersson, H. Nakatsuji, M. Caricato, X. Li, H.P. Hratchian, A.F. Izmaylov, J. Bloino, G. Zheng, J.L. Sonnenberg, M. Hada, M. Ehara, K. Toyota, R. Fukuda, J. Hasegawa, M. Ishida, T. Nakajima, Y. Honda, O. Kitao, H. Nakai, T. Vreven, J.A. Montgomery Jr., J.E. Peralta, F. Ogliaro, M. Bearpark, J.J. Heyd, E. Brothers, K.N. Kudin, V.N. Staroverov, R. Kobayashi, J. Normand, K. Raghavachari, A. Rendell, J.C. Burant, S.S. Iyengar, J. Tomasi, M. Cossi, N. Rega, J.M. Millam, M. Klene, J.E. Knox, J.B. Cross, V. Bakken, C. Adamo, J. Jaramillo, R. Gomperts, R.E. Stratmann, O. Yazyev, A.J. Austin, R. Cammi, C. Pomelli, J.W. Ochterski, R.L. Martin, K. Morokuma, V.G. Zakrzewski, G.A. Voth, P. Salvador, J.J. Dannenberg, S. Dapprich, A.D. Daniels, Ö. Farkas, J.B. Foresman, J.V. Ortiz, J. Cioslowski, D.J. Fox, *Gaussian 09, Revision A.02*, Gaussian, Inc, Wallingford, CT, 2009. `nkoccurfalse`
- [27] M.J. Frisch, G.W. Trucks, H.B. Schlegel, G.E. Scuseria, M.A. Robb, J.R. Cheeseman, G. Scalmani, V. Barone, B. Mennucci, G.A. Petersson, H. Nakatsuji, M. Caricato, X. Li, H.P. Hratchian, A.F. Izmaylov, J. Bloino, G. Zheng, J.L. Sonnenberg, M. Hada, M. Ehara, K. Toyota, R. Fukuda, J. Hasegawa, M. Ishida, T. Nakajima, Y. Honda, O. Kitao, H. Nakai, T. Vreven, J.A. Montgomery Jr., J.E. Peralta, F. Ogliaro, M. Bearpark, J.J. Heyd, E. Brothers, K.N. Kudin, V.N. Staroverov, R. Kobayashi, J. Normand, K. Raghavachari, A. Rendell, J.C. Burant, S.S. Iyengar, J. Tomasi, M. Cossi, N. Rega, J.M. Millam, M. Klene, J.E. Knox, J.B. Cross, V. Bakken, C. Adamo, J. Jaramillo, R. Gomperts, R.E. Stratmann, O. Yazyev, A.J. Austin, R. Cammi, C. Pomelli, J.W. Ochterski, R.L. Martin, K. Morokuma, V.G. Zakrzewski, G.A. Voth, P. Salvador, J.J. Dannenberg, S. Dapprich, A.D. Daniels, Ö. Farkas, J.B. Foresman, J.V. Ortiz, J. Cioslowski, D.J. Fox, *Gaussian 09, Revision A.02*, Gaussian, Inc, Wallingford, CT, 2009.
- [28] T.S. Singh, S. Mitra, A.K. Chandra, N. Tamai, S. Kar, *J. Photochem. Photobiol. A: Chem.* 197 (2008) 295–305.
- [29] S. Murali, W. Rettig, *J. Phys. Chem. A* 110 (2006) 28–37.
- [30] D. Jacquemin, T. Bahers, C. Adamo, I. Ciofini, *Phys. Chem. Chem. Phys.* 14 (2012) 5383–5388.